Chinese Journal of
POLYMER SCIENCE

RAPID COMMUNICATION

https://doi.org/10.1007/s10118-020-2435-5
Chinese J. Polym. Sci. **2020**, *38*, 797–805

Wide Band-gap Two-dimension Conjugated Polymer Donors with Different Amounts of Chlorine Substitution on Alkoxyphenyl Conjugated Side Chains for Non-fullerene Polymer Solar Cells

Youdi Zhang[a,c], Yong Wang[a], Ruijie Ma[b], Zhenghui Luo[b], Tao Liu[b*], So-Huei Kang[d], He Yan[b], Zhongyi Yuan[a,c], Changduk Yang[d*], and Yiwang Chen[a,c,e*]

[a] *College of Chemistry, Nanchang University, Nanchang 330031, China*
[b] *Department of Chemistry and Hong Kong Branch of Chinese National Engineering Research Center for Tissue Restoration & Reconstruction, Hong Kong University of Science and Technology (HKUST), Clear Water Bay, Kowloon, Hong Kong, China*
[c] *Institute of Polymers and Energy Chemistry (IPEC), Nanchang University, Nanchang 330031, China*
[d] *Ulsan National Institute of Science and Technology (UNIST), Ulsan, Republic of Korea*
[e] *Institute of Advanced Scientific Research (iASR), Jiangxi Normal University, Nanchang 330022, China*

Electronic Supplementary Information

Abstract In this study, wide bandgap (WBG) two-dimensional (2D) copolymer donors (**DZ1**, **DZ2**, and **DZ3**) based on benzodithiophene (BDT) on alkoxyphenyl conjugated side chains without and with different amounts of chlorine atoms and difluorobenzotriazole (FBTZ) are designed and synthesized successfully for efficient non-fullerene polymer solar cells (PSCs). Three polymer donors **DZ1**, **DZ2**, and **DZ3** display similar absorption spectra at 300–700 nm range with optional band-gap (E_g^{opt}) of 1.84, 1.92, and 1.97 eV, respectively. Compared with reported **DZ1** without chlorine substitution, it is found that introducing chlorine atoms into the *meta*-position of the alkoxyphenyl group affords polymer possessing a deeper the highest occupied molecular orbital (HOMO) energy level, which can increase open circuit voltage (V_{OC}) of PSCs, as well as improve hole mobility. Non-fullerene bulk heterojunction PSCs based on **DZ2**:MeIC demonstrate a relatively high power conversion efficiency (PCE) of 10.22% with a V_{OC} of 0.88 V, a short-circuit current density (J_{SC}) of 17.62 mA/cm^2, and a fill factor (FF) of 68%, compared with PSCs based on **DZ1**:MeIC (a PCE of 8.26%) and **DZ3**:MeIC (a PCE of 6.28%). The results imply that adjusting chlorine atom amount on alkoxyphenyl side chains based on BDT polymer donors is a promising approach of synthesizing electron-rich building block for high performance of PSCs.

Keywords Wide-bandgap copolymer; Organic solar cells; Polymer donors; Chlorine substitution; Nonfullerene polymer solar cells

Citation: Zhang, Y.; Wang, Y.; Ma, R.; Luo, Z.; Liu, T.; Kang, S. H.; Yan, H.; Yuan, Z.; Yang, C. ; Chen, Y. Wide band-gap two-dimension conjugated polymer donors with different amounts of chlorine substitution on alkoxyphenyl conjugated side chains for non-fullerene polymer solar cells. *Chinese J. Polym. Sci.* **2020**, *38*, 797–805.

INTRODUCTION

Polymer solar cells (PSCs) consist of a p-type conjugated polymer donor and an n-type organic semiconductor (including fullerene derivatives and non-fullerene organic semiconductors).[1–32] For the past few years, PSCs have been developed rapidly, exhibiting outstanding advantages such as simple device structure, low cost, lightweight, flexibility, and semitransparency.[33–36] Now, it has become a global frontier and hot spot in organic photovoltaic research, which mainly focuses on improving power conversion efficiency (PCE) and stability, reducing the cost of photovoltaic materials and device preparation, and subsequent industrialization and practical application.[37] PCEs of the single-junction solar cells have been over 16% according to reported studies so far.[38–43] Currently, typical polymer donors are mainly D-A type copolymers PBDB-T,[44] PM6,[45] J91,[46] P2F-EHp[47] with 2D conjugated side chains, and 2D polymer donors have more advantages such as extensive intramolecular conjugation, facilitated intermolecular interaction and π-π overlap, compared with 1D conjugated polymer donors. Meanwhile, acceptors are mainly n-type organic semiconductors. With regard to fullerene and its derivatives as acceptors for PSCs, fused-ring acceptors (some typical ones such as ITIC, Y6) feature good stability, easily tailored synthesis methods, strong absorption in the visible light region, and tunable energy levels, thus becoming more and more dominant in PSC research community. Excellent polymer donors usually contain complementary absorption spectra with above-mentioned acceptors, which is very important to build

* Corresponding authors, E-mail: liutaozhx@ust.hk (T.L.)
E-mail: yang@unist.ac.kr (C.D.Y.)
E-mail: ywchen@ncu.edu.cn (Y.W.C.)

Received March 5, 2020; Accepted March 24, 2020; Published online May 20, 2020

highly efficient organic photovoltaics.[48,49]

It is well known that donor materials need to match the energy level of the acceptors to obtain increased open-circuit voltages (V_{OC}s), and have a relatively strong absorption spectrum and morphological compatibility with the acceptors to increase short-circuit current densities (J_{SC}s) and fill factors (FFs) for PSCs. Benzodithiophene (BDT) is an excellent electron-donating donor unit with a large planar structure and outstanding crystallinity. Highly efficient PSCs generally include BDT units for D-A copolymer donors as electron-rich segments and A-D-A type small molecule donors or acceptors as conjugated core to build two-dimension (2D) excellent molecular systems.[50–53] In general, BDT unit based 2D conjugated photoelectronic materials show excellent photovoltaic performance in nonfullerene PSCs (NF-PSCs).[54] BDT unit with 2D conjugated side chains is adopted most widely by phenyl and thiophene substitution to tune energy levels and improve geomorphology of active layers.[51,55,56] In order to further improve the photovoltaic properties of PSCs, halogen atoms are introduced into 2D conjugated side chains to regulate molecular energy levels, charge transfer, and the compatibility of donor and acceptor, since halogenation is a very effective method for increasing the corresponding parameters of organic semiconductors. In recent years, fluorinated and chlorinated substituted photovoltaic materials (including donors and acceptors) have shown great potential in achieving highly efficient PSCs.[57–61] Hou's group studied systematically the effects of fluorinated and chlorinated donors and acceptors on the performance, and the results indicated that chlorination was more effective than fluorination in reducing molecular energy levels and broadening absorption spectra.[62,63] Zhang *et al*. introduced a fluorine atom into the thienyl conjugated side chain to synthesize the polymer donor PM6, which was measured with deeper HOMO levels and higher PCE.[51] Recently, Yan's group used polymer donor PM7 with chlorine atoms to replace fluorine atoms on thienyl side chains, which resulted in enhanced V_{OC}, when coping with acceptor Y6 achieving a PCE as much as 17% efficiency. PSCs based on BDT unit with conjugate side chains on phenyl group using chlorine substitution also obtain the excellent performance in reported literatures, and chlorinated polymer acquired the lower HOMO energy level as well as high V_{OC} and PCE.[64] Huang's group synthesized P2F-Ehp by introducing two fluorine atoms on phenyl substituted side chains and it was applied in PSCs, which achieved higher V_{OC} and PCE.[47] These results imply that chlorination may have greater potential for large-scale applications as it is more attractive to design low-cost photovoltaic materials.

In this study, we designed and synthesized WBG 2D copolymers **DZ1**, **DZ2**, and **DZ3** with different degrees of chlorine substitution by using difluorobenzotriazole (FBTZ) through Stille coupling polymerization (Scheme 1 and Scheme S1 in the electronic supplementary information, ESI). Three polymer donors **DZ1**, **DZ2**, and **DZ3** displayed broad absorption in the ultraviolet-visible light region of 300–700 nm with optional band-gap (E_g^{opt}) of 1.84, 1.92, and 1.97 eV, respectively. HOMO energy level of polymer donors **DZ2** and **DZ3** by introducing chlorine into the alkoxyphenyl group is deeper than that of reported **DZ1** without chlorine substitution, which can increase V_{OC} of PSCs, correlative charge carrier, compatibility of donor and acceptor, and photovoltaic performance.[56] Non-fullerere PSCs based on **DZ2** as the donor and MeIC[65] as the acceptor demonstrates a relatively high PCE of 10.22% with a V_{OC} of 0.88 V, a J_{SC} of 17.62 mA/cm^2, and a FF of 68%, compared with PSCs based on **DZ1**:MeIC (a PCE of 8.26%) and **DZ3**:MeIC (a PCE of 6.28%). The results suggest that introducing different numbers of chlorine atoms on alkoxyphenyl conjugated side chains based on BDT polymer donors is a vigorous strategy to synthesize electron-rich building block for high performance of PSCs.

RESULTS AND DISCUSSION

Synthesis and Characterization

The molecular structures of polymer donors **DZ1**, **DZ2**, **DZ3**, and acceptor MeIC are shown in Figs. 1(a) and 1(b). Three

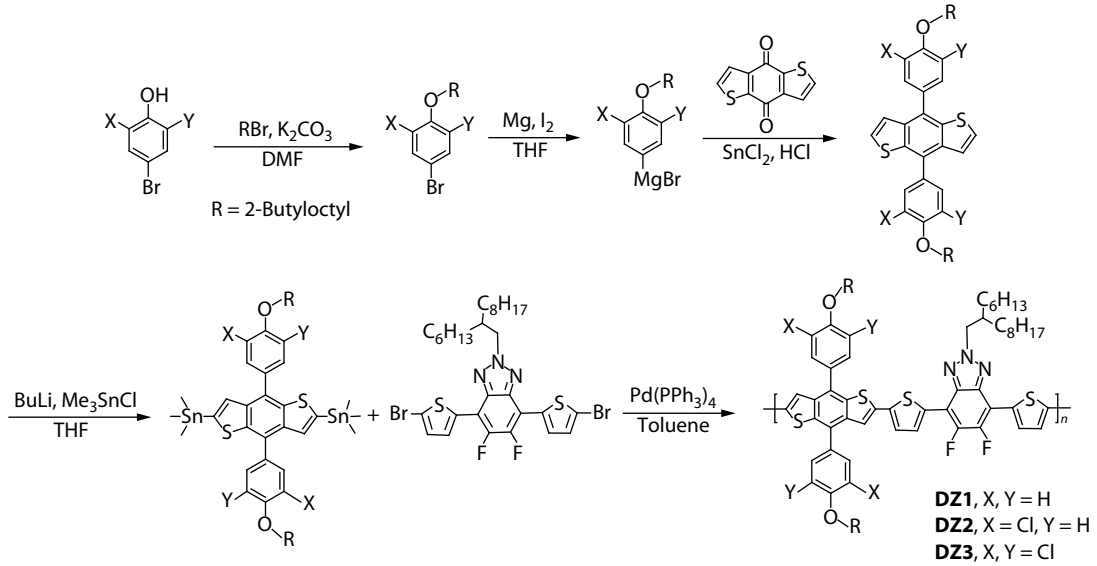

Scheme 1 Chemical structures and synthetic routes of **DZ1**, **DZ2**, and **DZ3**.

https://doi.org/10.1007/s10118-020-2435-5

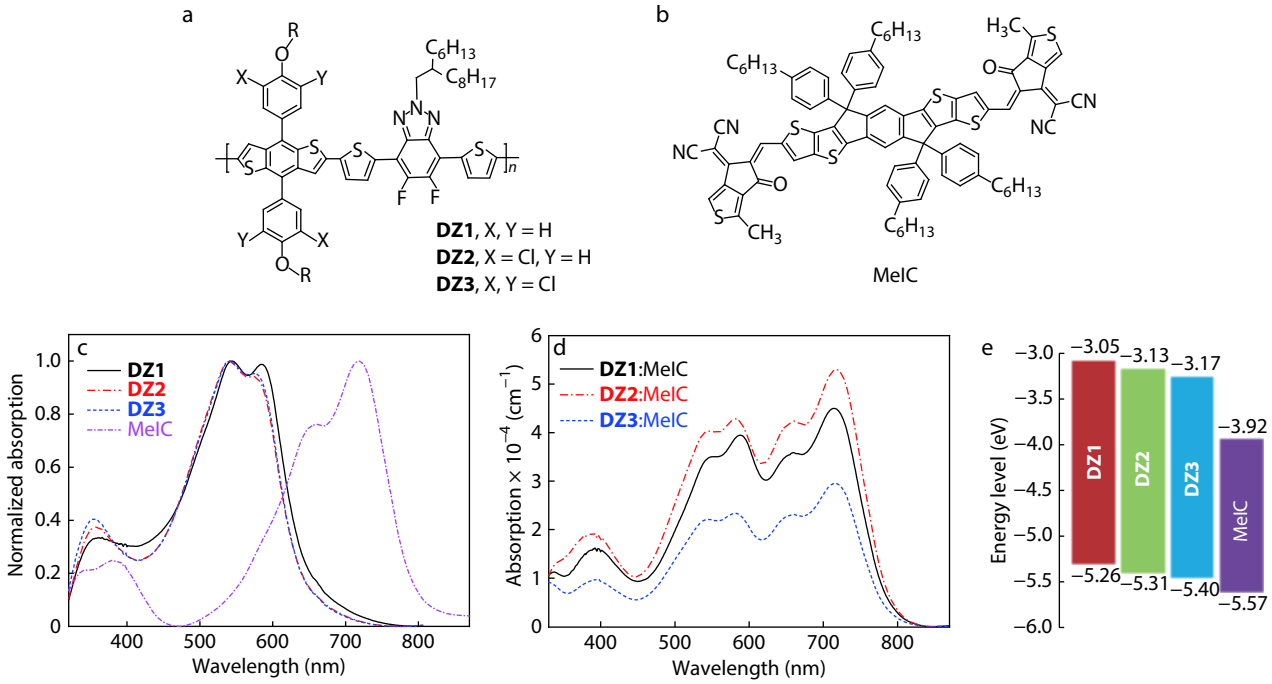

Fig. 1 (a) The chemical structure of **DZ1**, **DZ2**, and **DZ3**; (b) Chemical structure of MeIC; (c) Normalized absorption spectra of **DZ1**, **DZ2**, **DZ3**, and MeIC in film; (d) Normalized absorption spectra of **DZ1**:MeIC, **DZ2**:MeIC, and **DZ3**:MeIC in $CHCl_3$ solution; (e) The energy level diagram of donor and acceptors.

polymer donors were synthesized through the Stille coupling reaction using $Pd(PPh_3)_4$ as a catalyst and toluene as a reactive solvent. The detailed synthetic procedures and characterization methods of monomers and polymers are displayed in ESI. The high-temperature gel permeation chromatography was used to test the number-average molecular weight (M_n) and polydispersity index (PDI) of polymers **DZ1**, **DZ2**, and **DZ3**. M_n of polymer donors **DZ1**, **DZ2**, and **DZ3** was 15.3, 19.6, and 9.04 kDa with a PDI of 2.06, 2.20, and 3.10, respectively. The data were tested at 160 °C using polystyrene as a reference and 1,2,4-trichlorobenzene as the eluent. Three polymers showed good solubility in normal organic solvents, such as toluene, *o*-dichlorobenzene, chlorobenzene, and chloroform. Thermodynamic stability of the three polymers was measured by TGA in a nitrogen atmosphere at a rate of 10 °C/min. The decomposition temperatures (defined as the temperature of 5% weight loss) of polymers **DZ1**, **DZ2**, and **DZ3** were 359, 352, and 400 °C, respectively (Fig. S1a, in ESI). Fig. S1(b) (in ESI) shows differential scanning calorimetry (DSC) thermograms of three polymers **DZ1**, **DZ2**, and **DZ3**, which suggest no obvious crystalline peaks from 50 °C to 300 °C.

Optical and Electrochemical Properties

Fig. 1 and Fig. S2 (in ESI) show the UV-visible absorption spectra of three polymers in chloroform solution and as film, respectively. In solution, the absorption spectra of polymers **DZ2** and **DZ3** were slightly red-shifted, and displayed the strong *π-π* stacking. And three polymers showed a similar intramolecular charge transfer (ICT) peak at around 532 nm. In the solid film, by comparison with polymer **DZ1**, the absorption spectra of **DZ2** and **DZ3** were slightly blue-shifted and narrow (Fig. 1c). And the absorption maxima of all polymers were at 538, 540, and 542 nm, respectively. The absorption edges of the three donors were at 647, 629, and 640 nm with the corresponding optical bandgap (E_g) of 1.84, 1.92, and 1.97 eV, respectively (Table 1). Such a blueshift phenomenon expended the main absorption region, which would enable the greater complementary light-harvesting spectrum to produce higher J_{SC} and PCE values. The absorption maximum and absorption edge of the acceptor MeIC were 718 and 795 nm, respectively. The UV-visible absorption spectra of three polymer blends with acceptor MeIC are shown in Fig. 1(d). The blend film absorption intensity (ε) exhibited the following order: **DZ2**:MeIC (5.30×10^4 cm^{-1}) > **DZ1**:MeIC (4.50×10^4 cm^{-1}) > **DZ3**:MeIC (2.95×10^4 cm^{-1}), as outlined in Table 1. It was obvious that **DZ2**:MeIC obtained the strongest absorption coefficient among the three blends. The result is consistent with the J_{SC} discussed below. The hole mobilities of three polymers were measured by using space charge limited current (SCLC) method, as shown in Fig.

Table 1 Optical properties, electronic energy levels and hole mobilities of **DZ1**, **DZ2**, and **DZ3**.

Donor	T_d (°C)	λ_{max}^{sol} (nm)	λ_{max}^{film} (nm)	E_g [a] (eV)	ε [b] $\times 10^{-4}$ (cm^{-1})	HOMO [c] (eV)	LUMO [c] (eV)	μ_h ($cm^2 \cdot V^{-1} \cdot s^{-1}$)
DZ1	359	535	538	1.84	4.50	−5.26	−3.05	7.56×10^{-4}
DZ2	352	531	540	1.92	5.30	−5.32	−3.13	8.43×10^{-4}
DZ3	400	533	542	1.97	2.95	−5.40	−3.17	9.64×10^{-4}

[a] Estimated from the absorption edge in film; [b] Molar absorptivity at λ_{max} in blended films; [c] Measured from the cyclic voltammograms.

https://doi.org/10.1007/s10118-020-2435-5

S3 (in ESI). Polymer donors **DZ2** and **DZ3** exhibited higher hole mobility (8.43×10^{-4} and 9.64×10^{-4} $cm^2 \cdot V^{-1} \cdot s^{-1}$) than **DZ1** ($7.56 \times 10^{-4}$ $cm^2 \cdot V^{-1} \cdot s^{-1}$) (Table 1). Such high mobility of neat films may be ascribed to the introduction of chlorine atoms, which resulted in the stronger molecular interaction to improve more effective charge transport.

The electrochemical properties of three polymer donors were measured by cyclic voltammetry (CV) using the standard three electrode electrochemical cell. The energy level diagram and the CV curves of the three polymers are shown in Fig. 1(e) and Fig. S4 (in ESI). According to the formula: $E_{HOMO} = -e(E_{ox} + 4.71)$ (eV) and $E_{LUMO} = -e(E_{red} + 4.71)$ (eV), the highest occupied molecular orbitals (HOMOs) and the lowest unoccupied molecular orbitals (LUMOs) were calculated, respectively. The HOMO energy levels of the three polymer donors were measured as −5.26, −5.32, and −5.40 eV, respectively. The corresponding LUMO energy levels were −3.05, −3.13, and −3.17 eV, respectively. The HOMOs and LUMOs of polymers **DZ1**, **DZ2**, and **DZ3** were consistent with the results of DFT calculation with the HOMO/LUMO of −4.86/−2.78 eV for **DZ1**, −5.05/−2.94 eV for **DZ2**, and −5.19/−3.05 eV for **DZ3** (Fig. S5, in ESI). Obviously, the HOMO energy level of polymer **DZ3** with four chlorinated substitutions was deeper than those of polymers **DZ1** without chlorinated substitution and **DZ2** with two chlorinated substitutions, which was beneficial to obtaining a high V_{OC} value. Besides, the strategy demonstrated that chlorine atom was a stronger electron-withdrawing group, generating the deeper HOMO energy levels. And the trend is similar to the reported literature with fluorinated and trifluoromethyl substitution on phenyl conjugated side chains. These results implied that chlorinated substitution is a promising approach of achieving deeper HOMO energy levels to increase V_{OC} for efficient NF-PSCs.

Theoretical Calculations

Theoretical calculations were performed by adopting density functional theory (DFT) with the B3LYP/6-31G (d, p) basis set. To simplify the calculation procedure, long alkyl chains were changed to methyl groups. As shown in Fig. S5 (in ESI), HOMO surface of the polymers was delocalized on both BDT and FBTZ segments. Nevertheless, LUMO surface of the polymers was more localized on the acceptor units, demonstrating that FBTZ unit displayed strong electron-withdrawing character. In addition, three polymeric skeletons exhibited good planar and linear construction, as well as a predominant homogeneous dispersion of positive electrostatic potential (ESP), which is beneficial to obtaining high charge carrier mobilities (Fig. 2). As illustrated in Fig. 2, the optimal molecular configuration of polymer **DZ2** is that the asymmetrical side chains with two chlorine substitutions on phenyl groups were located on the two sides of the molecule plane, which is different from polymers **DZ1** and **DZ3** without and with the symmetrical chlorine substitution conjugated side chains, generating the different molecular arrangement and dipole moments. Polymer **DZ2** with two chlorine substitutions on the phenyl conjugated side chains obtained the dipole moment value of 8.81 D, being superior to that of **DZ1** (5.43 D) and **DZ3** (3.15 D). The result indicates that the orientation of the dipole moment would force polymer **DZ2** to enlarge the accumulation area and intensity.[66–68]

Photovoltaic Properties

The photovoltaic performance of polymer donors **DZ1**, **DZ2**, and **DZ3** was studied by fabricating NF-PSCs with MeIC as an acceptor and **DZ1** or **DZ2** or **DZ3** as a donor with the conventional device architecture of ITO/PEDOT:PSS/photovoltaic active layer/Zracac/Al, where ITO is indium tin oxide, PEDOT is poly(3,4-ethylenedioxythiophene), PSS is poly(styrene sulfonate), and Zracac is zirconium(IV) acetylaceton. Fig. 3(a) depicts the current density-voltage (*J-V*) plots of the devices with the best performance. The corresponding device parameters with J_{SC}, V_{OC}, FF, and PCE are outlined in Table 2. The PSC based on **DZ1**:MeIC obtained a PCE of 8.262%, a V_{OC} of 0.814, a FF of 0.667, and a J_{SC} of 15.237 $mA \cdot cm^{-2}$. PCE of 10.215% based on **DZ2**:MeIC blend with V_{OC} of 0.877, FF of 0.684, and J_{SC} of

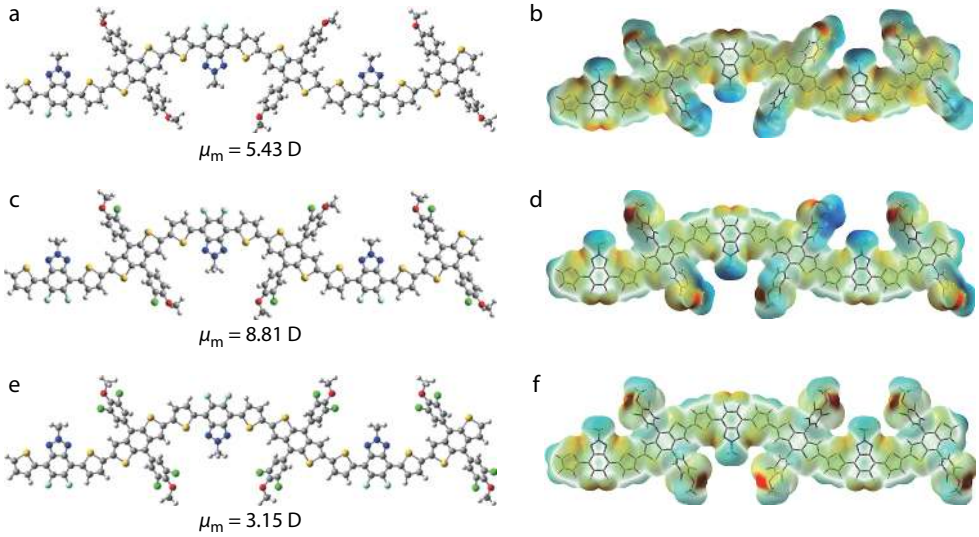

Fig. 2 Optimized geometries of polymers **DZ1**, **DZ2**, and **DZ3** by DFT at the B3LYP/6-31G (d, p) level. (a, c, e) Side view and (b, d, f) map of the DFT electrostatic potential (ESP) surface of **DZ1**, **DZ2**, and **DZ3**, respectively. Cyan color indicates greater negative charge, while yellow and red colors indicate positive charges.

https://doi.org/10.1007/s10118-020-2435-5

17.061 mA·cm^{-2} is higher that of **DZ3**:MeIC (PCE of 5.966%, V_{OC} of 1.000, FF of 0.609, and J_{SC} of 10.311 mA·cm^{-2}). It is obvious that V_{OC} of the **DZ3**:MeIC-based PSC was the highest due to the deeper HOMO energy level of polymer **DZ3**. Furthermore, a device based on **DZ2**:MeIC achieved the optimized efficiency of photovoltaic performance, which was attributed to the balanced charge transport below discussed mobilities. The result suggested that introducing suitable chlorine amount on phenyl conjugated side chains could obtain the increments of J_{SC}, V_{OC}, FF, and PCE.

Charge Carrier Mobilities

In order to better understand the effect of internal charge carriers on the photovoltaic properties of NF-PSCs, the charge mobility measurements of the neat polymer donors **DZ1**, **DZ2**, and **DZ3**, and the polymer blends of **DZ1**:MeIC, **DZ2**:MeIC, and **DZ3**:MeIC were carried out by adopting the space-charge-limited current (SCLC) method with a device structure of ITO/PEDOT:PSS/active layer/MoO_3/Al for the hole mobility (μ_h) and ITO/ZnO/active layer/Zracac/Al for the electron mobility (μ_e). The current-voltage curves of mobilities are exhibited in Fig. 4. It can be seen from Table 2 that the hole mobilities of **DZ1**:MeIC, **DZ2**:MeIC, and **DZ3**:MeIC blends were 6.12 × 10^{-4}, 6.78 × 10^{-4}, and 7.36 × 10^{-4} cm^2·V^{-1}·s^{-1}, respectively. The electron mobility of **DZ2**:MeIC blend (3.74 × 10^{-4} cm^2·V^{-1}·s^{-1}) was higher than those of **DZ1**:MeIC (3.02 × 10^{-4} cm^2·V^{-1}·s^{-1}), and **DZ3**:MeIC blends (3.34 × 10^{-4} cm^2·V^{-1}·s^{-1}). And the specific value of hole and electron mobility of **DZ2**:MeIC blend (μ_h/μ_e = 1.81) was more balanced than that of **DZ1**:MeIC (μ_h/μ_e = 2.00) and **DZ3**:MeIC blends (μ_h/μ_e = 2.20) (Table 2). The result demonstrates

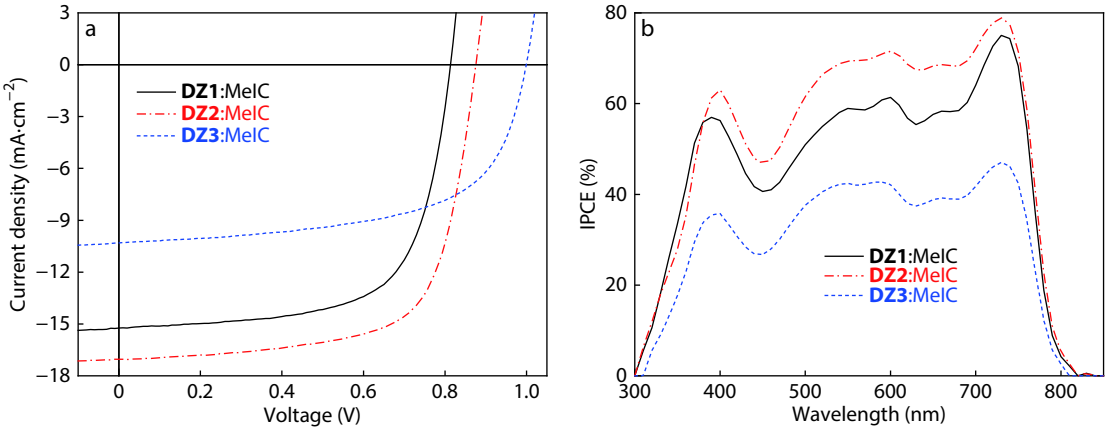

Fig. 3 (a) *J-V* characteristics of the best OSCs under the illumination of AM 1.5G, 100 mW·cm^{-2}; (b) IPCE spectra of the devices based on **DZ1**:MeIC, **DZ2**:MeIC, and **DZ3**:MeIC.

Table 2 Photovoltaic data of the donors:MeIC (1:1, *W*:*W*)-based OSCs.

Donor	V_{OC} (V)	J_{SC} (mA·cm^{-2})	Calcd. J_{SC} (mA·cm^{-2})	FF (%)	PCE [a] (%)	$\mu_h \times 10^4$ (cm^2·V^{-1}·s^{-1})	$\mu_e \times 10^4$ (cm^2·V^{-1}·s^{-1})	μ_h/μ_e
DZ1	0.810 ± 0.010 (0.814)	15.010 ± 0.211 (15.237)	14.530	0.653 ± 0.007 (0.667)	7.939 ± 0.19 (8.262)	6.12	3.02	2.00
DZ2	0.872 ± 0.008 (0.877)	16.911 ± 0.231 (17.061)	16.688	0.677 ± 0.010 (0.684)	9.983 ± 0.20 (10.215)	6.78	3.74	1.81
DZ3	0.998 ± 0.011 (1.000)	9.997 ± 0.228 (10.311)	9.763	0.598 ± 0.006 (0.609)	5.77 ± 0.20 (5.966)	7.36	3.34	2.20

[a] Average values and standard deviation are calculated from 20 devices. The values in parentheses belong to the best device.

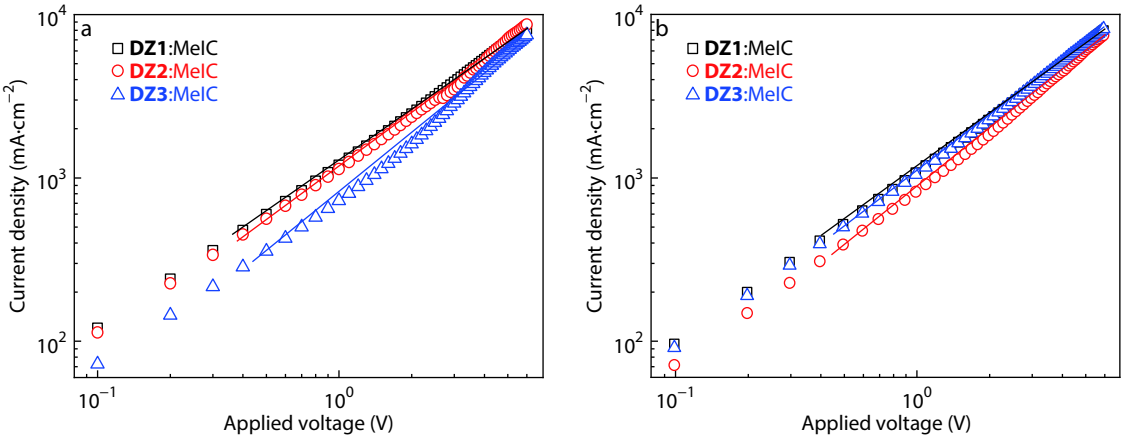

Fig. 4 $J^{0.5}$-V ($V = V_{appl} - V_{bi} - V_s$) characteristics of (a) the hole-only devices (ITO/PEDOT:PSS/active layer/MoO_3/Al) and (b) the electron-only devices (ITO/ZnO/active layer/Zracac/Al).

https://doi.org/10.1007/s10118-020-2435-5

that a better balance charge mobility was achieved by **DZ2** based system, which could contribute to its higher FF value.

Morphology Study

The optimized geomorphology is important to enhance the photovoltaic performance of PSCs. To further gain insight into the morphology of the photovoltaic layers, atomic force microscopy (AFM) was implemented. As shown in Fig. S6 (in ESI), the AFM images of neat **DZ1**, **DZ2**, and **DZ3** films revealed that the root mean square (RMS) values of neat **DZ1**, **DZ2**, and **DZ3** films were 1.00, 1.10, and 1.32 nm, respectively. Fig. 5 shows the AFM images of **DZ1**:MeIC, **DZ2**:MeIC, and **DZ3**:MeIC blends. The arranged order of surface roughness of blends was **DZ1**:MeIC < **DZ2**:MeIC < **DZ3**:MeIC, and the corresponding RMS values were 1.34, 2.10, and 2.89 nm, respectively. The result implied that the suitable surface roughness was crucial to enhancing the efficiency of PSCs.

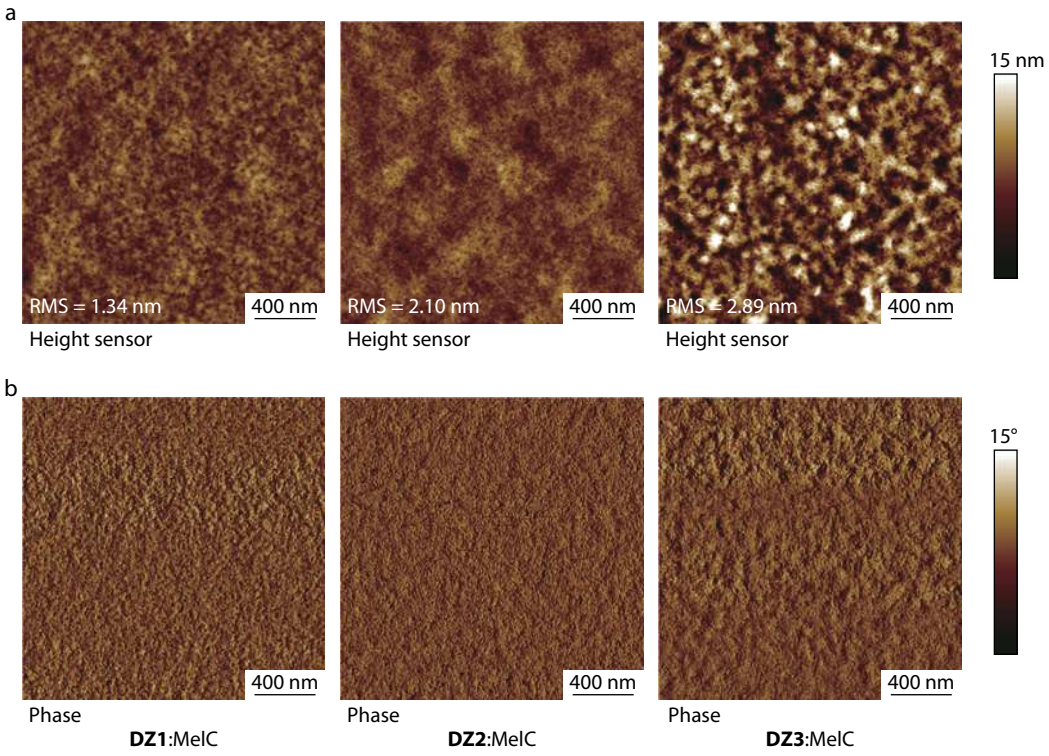

Fig. 5 AFM (a) height images and (b) phase images of **DZ1**:MeIC, **DZ2**:MeIC, and **DZ3**:MeIC blends.

CONCLUSIONS

In summary, we have successfully designed and synthesized new WBG 2D copolymer donors **DZ1**, **DZ2**, and **DZ3** without and with different degrees of chlorination for application in NF-PSCs. These 2D conjugated polymer donors exhibited the broad absorption spectra in the UV-visible light region and its absorption spectra were well complementary with that of acceptor MeIC. Polymers **DZ2** and **DZ3** displayed deeper HOMO energy levels, compared with polymer **DZ1**, and generated the higher V_{OC} value. The NF-PSCs based on **DZ2**:MeIC with two chlorinated substitutions achieved an optimized PCE of 10.215% with V_{OC} of 0.877, FF of 0.684, and J_{SC} of 17.061 mA·cm^{-2}, which was superior to those of **DZ1**:MeIC (PCE = 8.262%) and **DZ3**:MeIC (PCE = 5.966%). More balanced charge carrier mobilities and suitable surface roughness are consistent with the best device condition of NF-PSCs based on **DZ2**:MeIC. Obviously, these BDT unit-based-chlorinated polymers significantly enhanced the photovoltaic performance of NF-PSCs. In addition, we revealed the close-knit relationship between the molecular structure with chlorinated substitution and device properties. This study implies that appropriately introducing chlorine atoms on alkoxyphenyl side chains based on BDT polymer donors was a feasible strategy for efficient NF-PSCs.

Electronic Supplementary Information

Electronic supplementary information (ESI) is available free of charge in the online version of this article at https://doi.org/10.1007/s10118-020-2435-5.

ACKNOWLEDGMENTS

This work was financially supported by the National Natural Science Foundation of China (Nos. 51763017, 21602150, 51425304, 51863012, 21861025, and 51833004), the Shen Zhen Technology and Innovation Commission (Nos. JCYJ20170413173814007 and JCYJ20170818113905024), the Hong Kong Research Grants Council (Research Impact Fund R6021-18, Nos. 16305915, 16322416, 606012, and 16303917), Hong Kong Innovation and Technology Commission for the support through projects ITC-CNERC14SC01 and ITS/471/18, the

National Research Foundation of Korea (NRF) grant funded by the Korea government (MSIP) (No. 2018R1A2A1A05077194), Wearable Platform Materials Technology Center (WMC; No. 2016R1A5A1009926) funded by the National Research Foundation of Korea (NRF) Grant by the Korean Government (MSIT), and the Research Project Funded by Ulsan City (No. 1.200042) of UNIST (Ulsan National Institute of Science & Technology).

REFERENCES

1 Li, Y. Molecular design of photovoltaic materials for polymer solar cells: toward suitable electronic energy levels and broad absorption. *Acc. Chem. Res.* **2012**, *45*, 723–733.
2 Guo, X.; Facchetti, A.; Marks, T. J. Imide- and amide-functionalized polymer semiconductors. *Chem. Rev.* **2014**, *114*, 8943–9021.
3 Yan, C.; Barlow, S.; Wang, Z.; Yan, H.; Jen, A. K. Y.; Marder, S. R.; Zhan, X. Non-fullerene acceptors for organic solar cells. *Nat. Rev. Mater.* **2018**, *3*, 18003.
4 Liu, T.; Zhang, Y.; Shao, Y.; Ma, R.; Luo, Z.; Xiao, Y.; Yang, T.; Lu, X.; Yuan, Z.; Yan, H.; Chen, Y.; Li, Y. Asymmetric acceptors with fluorine and chlorine substitution for organic solar cells toward 16.83% efficiency. *Adv. Funct. Mater.* **2020**, *32*, 2000456.
5 Cui, C.; Li, Y. High-performance conjugated polymer donor materials for polymer solar cells with narrow-bandgap nonfullerene acceptors. *Energy Environ. Sci.* **2019**, *12*, 3225–3246.
6 Genene, Z.; Mammo, W.; Wang, E.; Andersson, M. R. Recent advances in n-type polymers for all-polymer solar cells. *Adv. Mater.* **2019**, *31*, 1807275.
7 Luo, Z.; Liu, T.; Chen, Z.; Xiao, Y.; Zhang, G.; Huo, L.; Zhong, C.; Lu, X.; Yan, H.; Sun, Y.; Yang, C. Isomerization of perylene diimide based acceptors enabling high-performance nonfullerene organic solar cells with excellent fill factor. *Adv. Sci.* **2019**, *6*, 1802065.
8 Hou, J.; Inganäs, O.; Friend, R. H.; Gao, F. Organic solar cells based on non-fullerene acceptors. *Nat. Mater.* **2018**, *17*, 119–128.
9 Zhao, C.; Wang, J.; Jiao, J.; Huang, L.; Tang, J. Recent advances of polymer acceptors for high-performance organic solar cells. *J. Mater. Chem. C* **2020**, *8*, 28–43.
10 Liu, T.; Xue, X.; Huo, L.; Sun, X.; An, Q.; Zhang, F.; Russell, T. P.; Liu, F.; Sun, Y. Highly efficient parallel-like ternary organic solar cells. *Chem. Mater.* **2017**, *29*, 2914–2920.
11 Ma, R.; Chen, Y.; Liu, T.; Xiao, Y.; Luo, Z.; Zhang, M.; Luo, S.; Lu, X.; Zhang, G.; Li, Y.; Yan, H.; Chen, K. Improving the performance of near infrared binary polymer solar cells by adding a second non-fullerene intermediate band-gap acceptor. *J. Mater. Chem. C* **2020**, *8*, 909–915.
12 Huang, C.; Liao, X.; Gao, K.; Zuo, L.; Lin, F.; Shi, X.; Li, C. Z.; Liu, H.; Li, X.; Liu, F.; Chen, Y.; Chen, H.; Jen, A. K. Y. Highly efficient organic solar cells based on S, N-heteroacene non-fullerene acceptors. *Chem. Mater.* **2018**, *30*, 5429–5434.
13 Baran, D.; Ashraf, R. S.; Hanifi, D. A.; Abdelsamie, M.; Gasparini, N.; Röhr, J. A.; Holliday, S.; Wadsworth, A.; Lockett, S.; Neophytou, M.; Emmott, C. J. M.; Nelson, J.; Brabec, C. J.; Amassian, A.; Salleo, A.; Kirchartz, T.; Durrant, J. R.; McCulloch, I. Reducing the efficiency-stability-cost gap of organic photovoltaics with highly efficient and stable small molecule acceptor ternary solar cells. *Nat. Mater.* **2017**, *16*, 363–369.
14 He, Q.; Shahid, M.; Wu, J.; Jiao, X.; Eisner, F. D.; Hodsden, T.; Fei, Z.; Anthopoulos, T. D.; McNeill, C. R.; Durrant, J. R.; Heeney, M. Fused cyclopentadithienothiophene acceptor enables ultrahigh short-circuit current and high efficiency >11% in as-cast organic solar cells. *Adv. Funct. Mater.* **2019**, *29*, 1904956.
15 Yu, Z. P.; Liu, Z. X.; Chen, F. X.; Qin, R.; Lau, T. K.; Yin, J. L.; Kong, X.; Lu, X.; Shi, M.; Li, C. Z.; Chen, H. Simple non-fused electron acceptors for efficient and stable organic solar cells. *Nat. Commun.* **2019**, *10*, 2152.
16 Liu, T.; Guo, Y.; Yi, Y.; Huo, L.; Xue, X.; Sun, X.; Fu, H.; Xiong, W.; Meng, D.; Wang, Z.; Liu, F.; Russell, T. P.; Sun, Y. Ternary organic solar cells based on two compatible nonfullerene acceptors with power conversion efficiency >10%. *Adv. Mater.* **2016**, *28*, 10008–10015.
17 Feng, H.; Yi, Y. Q. Q.; Ke, X.; Yan, J.; Zhang, Y.; Wan, X.; Li, C.; Zheng, N.; Xie, Z.; Chen, Y. New anthracene-fused nonfullerene acceptors for high-efficiency organic solar cells: energy level modulations enabling match of donor and acceptor. *Adv. Energy Mater.* **2019**, *9*, 1803541.
18 Zhang, B.; Yu, Y.; Zhou, J.; Wang, Z.; Tang, H.; Xie, S.; Xie, Z.; Hu, L.; Yip, H. L.; Ye, L.; Ade, H.; Liu, Z.; He, Z.; Duan, C.; Huang, F.; Cao, Y. 3,4-Dicyanothiophene—a versatile building block for efficient nonfullerene polymer solar cells. *Adv. Energy Mater.* **2020**, 1904247.
19 Li, J.; Liang, Z.; Li, X.; Li, H.; Wang, Y.; Qin, J.; Tong, J.; Yan, L.; Bao, X.; Xia, Y. Insights into excitonic dynamics of terpolymer-based high-efficiency nonfullerene polymer solar cells: enhancing the yield of charge separation states. *ACS Appl. Mater. Interfaces* **2020**, *12*, 8475–8484.
20 Liu, T.; Luo, Z.; Fan, Q.; Zhang, G.; Zhang, L.; Gao, W.; Guo, X.; Ma, W.; Zhang, M.; Yang, C.; Li, Y.; Yan, H. Use of two structurally similar small molecular acceptors enabling ternary organic solar cells with high efficiencies and fill factors. *Energy Environ. Sci.* **2018**, *11*, 3275–3282.
21 Li, J.; Wang, Y.; Liang, Z.; Qin, J.; Ren, M.; Tong, J.; Yang, C.; Yang, C.; Bao, X.; Xia, Y. Non-toxic green food additive enables efficient polymer solar cells through adjusting the phase composition distribution and boosting charge transport. *J. Mater. Chem. C* **2020**, *8*, 2483–2490.
22 Sun, H.; Liu, T.; Yu, J.; Lau, T. K.; Zhang, G.; Zhang, Y.; Su, M.; Tang, Y.; Ma, R.; Liu, B.; Liang, J.; Feng, K.; Lu, X.; Guo, X.; Gao, F.; Yan, H. A monothiophene unit incorporating both fluoro and ester substitution enabling high-performance donor polymers for non-fullerene solar cells with 16.4% efficiency. *Energy Environ. Sci.* **2019**, *12*, 3328–3337.
23 Chao, P.; Chen, H.; Zhu, Y.; Lai, H.; Mo, D.; Zheng, N.; Chang, X.; Meng, H.; He, F. A benzo[1,2-*b*:4,5-*c*']dithiophene-4,8-dione-based polymer donor achieving an efficiency over 16%. *Adv. Mater.* **2020**, 1907059.
24 Liu, T.; Luo, Z.; Chen, Y.; Yang, T.; Xiao, Y.; Zhang, G.; Ma, R.; Lu, X.; Zhan, C.; Zhang, M.; Yang, C.; Li, Y.; Yao, J.; Yan, H. A nonfullerene acceptor with a 1000 nm absorption edge enables ternary organic solar cells with improved optical and morphological properties and efficiencies over 15%. *Energy Environ. Sci.* **2019**, *12*, 2529–2536.
25 Li, G.; Yang, W.; Wang, S.; Liu, T.; Yan, C.; Li, G.; Zhang, Y.; Li, D.; Wang, X.; Hao, P.; Li, J.; Huo, L.; Yan, H.; Tang, B. Methane-perylene diimide-based small molecule acceptors for high efficiency non-fullerene organic solar cells. *J. Mater. Chem. C* **2019**, *7*, 10901–10907.
26 Liao, Q.; Sun, H.; Li, B.; Guo, X. 26 mA cm^{-2} J_{SC} achieved in the integrated solar cells. *Sci. Bull.* **2019**, *64*, 1747–1749.
27 Zhang, Y.; Guo, X.; Guo, B.; Su, W.; Zhang, M.; Li, Y. Nonfullerene polymer solar cells based on a perylene monoimide acceptor with a high open-circuit voltage of 1.3 V. *Adv. Funct. Mater.* **2017**, *27*, 1603892.
28 Luo, Z.; Sun, R.; Zhong, C.; Liu, T.; Zhang, G.; Zou, Y.; Jiao, X.; Min, J.; Yang, C. Altering alkyl-chains branching positions for boosting the performance of small-molecule acceptors for highly efficient nonfullerene organic solar cells. *Sci. China Chem.* **2020**, *63*, 361–369.

29 An, Q.; Zhang, J.; Gao, W.; Qi, F.; Zhang, M.; Ma, X.; Yang, C.; Huo, L.; Zhang, F. Efficient ternary organic solar cells with two compatible non-fullerene materials as one alloyed acceptor. *Small* **2018**, *14*, 1802983.

30 Chen, H.; Hu, D.; Yang, Q.; Gao, J.; Fu, J.; Yang, K.; He, H.; Chen, S.; Kan, Z.; Duan, T.; Yang, C.; Ouyang, J.; Xiao, Z.; Sun, K.; Lu, S. All-small-molecule organic solar cells with an ordered liquid crystalline donor. *Joule* **2019**, *3*, 3034–3047.

31 Luo, Z.; Liu, T.; Xiao, Y.; Yang, T.; Chen, Z.; Zhang, G.; Zhong, C.; Ma, R.; Chen, Y.; Zou, Y. Significantly improving the performance of polymer solar cells by the isomeric ending-group based small molecular acceptors: insight into the isomerization. *Nano Energy* **2019**, *66*, 104146.

32 Feng, L.; Yuan, J.; Zhang, Z.; Peng, H.; Zhang, Z. G.; Xu, S.; Liu, Y.; Li, Y.; Zou, Y. Thieno[3,2-*b*]pyrrolo-fused pentacyclic benzotriazole-based acceptor for efficient organic photovoltaics. *ACS Appl. Mater. Interfaces* **2017**, *9*, 31985–31992.

33 Brus, V. V.; Lee, J.; Luginbuhl, B. R.; Ko, S. J.; Bazan, G. C.; Nguyen, T. Q. Solution-processed semitransparent organic photovoltaics: from molecular design to device performance. *Adv. Mater.* **2019**, *31*, 1900904.

34 Chen, S.; Jung, S.; Cho, H. J.; Kim, N. H.; Jung, S.; Xu, J.; Oh, J.; Cho, Y.; Kim, H.; Lee, B.; An, Y.; Zhang, C.; Xiao, M.; Ki, H.; Zhang, Z. G.; Kim, J. Y.; Li, Y.; Park, H.; Yang, C. Highly flexible and efficient all-polymer solar cells with high-viscosity processing polymer additive toward potential of stretchable devices. *Angew. Chem. Int. Ed.* **2018**, *57*, 13277–13282.

35 Fan, Q.; Su, W.; Chen, S.; Kim, W.; Chen, X.; Lee, B.; Liu, T.; Mé ndez-Romero, U. A.; Ma, R.; Yang, T.; Zhuang, W.; Li, Y.; Li, Y.; Kim, T. S.; Hou, L.; Yang, C.; Yan, H.; Yu, D.; Wang, E. Mechanically robust all-polymer solar cells from narrow band gap acceptors with hetero-bridging atoms. *Joule* **2020**, *4*, 658–672.

36 Xia, R.; Brabec, C. J.; Yip, H. L.; Cao, Y. High-throughput optical screening for efficient semitransparent organic solar cells. *Joule* **2019**, *3*, 2241–2254.

37 Du, X.; Heumueller, T.; Gruber, W.; Classen, A.; Unruh, T.; Li, N.; Brabec, C. J. Efficient polymer solar cells based on non-fullerene acceptors with potential device lifetime approaching 10 years. *Joule* **2019**, *3*, 215–226.

38 Sun, R.; Wu, Q.; Guo, J.; Wang, T.; Wu, Y.; Qiu, B.; Luo, Z.; Yang, W.; Hu, Z.; Guo, J.; Shi, M.; Yang, C.; Huang, F.; Li, Y.; Min, J. A layer-by-layer architecture for printable organic solar cells overcoming the scaling lag of module efficiency. *Joule* **2020**, *4*, 407–419.

39 Sun, C.; Qin, S.; Wang, R.; Chen, S.; Pan, F.; Qiu, B.; Shang, Z.; Meng, L.; Zhang, C.; Xiao, M.; Yang, C.; Li, Y. High efficiency polymer solar cells with efficient hole transfer at zero highest occupied molecular orbital offset between methylated polymer donor and brominated acceptor. *J. Am. Chem. Soc.* **2020**, *142*, 1465–1474.

40 Sun, C.; Pan, F.; Chen, S.; Wang, R.; Sun, R.; Shang, Z.; Qiu, B.; Min, J.; Lv, M.; Meng, L.; Zhang, C.; Xiao, M.; Yang, C.; Li, Y. Achieving fast charge separation and low nonradiative recombination loss by rational fluorination for high-efficiency polymer solar cells. *Adv. Mater.* **2019**, *31*, 1905480.

41 Cui, Y.; Yao, H.; Zhang, J.; Zhang, T.; Wang, Y.; Hong, L.; Xian, K.; Xu, B.; Zhang, S.; Peng, J.; Wei, Z.; Gao, F.; Hou, J. Over 16% efficiency organic photovoltaic cells enabled by a chlorinated acceptor with increased open-circuit voltages. *Nat. Commun.* **2019**, *10*, 2515.

42 Hong, L.; Yao, H.; Wu, Z.; Cui, Y.; Zhang, T.; Xu, Y.; Yu, R.; Liao, Q.; Gao, B.; Xian, K.; Woo, H. Y.; Ge, Z.; Hou, J. Eco-compatible solvent-processed organic photovoltaic cells with over 16% efficiency. *Adv. Mater.* **2019**, *31*, 1903441.

43 Cui, Y.; Yao, H.; Hong, L.; Zhang, T.; Tang, Y.; Lin, B.; Xian, K.; Gao, B.; An, C.; Bi, P.; Ma, W.; Hou, J. 17% Efficiency organic photovoltaic cell with superior processability. *Natl. Sci. Rev.* **2020**, DOI: 10.1093/nsr/nwz200.

44 Qian, D.; Ye, L.; Zhang, M.; Liang, Y.; Li, L.; Huang, Y.; Guo, X.; Zhang, S.; Tan, Z. A.; Hou, J. Design, application, and morphology study of a new photovoltaic polymer with strong aggregation in solution state. *Macromolecules* **2012**, *45*, 9611–9617.

45 Zhao, W.; Li, S.; Yao, H.; Zhang, S.; Zhang, Y.; Yang, B.; Hou, J. Molecular optimization enables over 13% efficiency in organic solar cells. *J. Am. Chem. Soc.* **2017**, *139*, 7148–7151.

46 Xue, L.; Yang, Y.; Xu, J.; Zhang, C.; Bin, H.; Zhang, Z. G.; Qiu, B.; Li, X.; Sun, C.; Gao, L.; Yao, J.; Chen, X.; Yang, Y.; Xiao, M.; Li, Y. Side chain engineering on medium bandgap copolymers to suppress triplet formation for high-efficiency polymer solar cells. *Adv. Mater.* **2017**, *29*, 1703344.

47 Fan, B.; Du, X.; Liu, F.; Zhong, W.; Ying, L.; Xie, R.; Tang, X.; An, K.; Xin, J.; Li, N.; Ma, W.; Brabec, C. J.; Huang, F.; Cao, Y. Fine-tuning of the chemical structure of photoactive materials for highly efficient organic photovoltaics. *Nat. Energy* **2018**, *3*, 1051–1058.

48 Lin, Y.; Wang, J.; Zhang, Z. G.; Bai, H.; Li, Y.; Zhu, D.; Zhan, X. An electron acceptor challenging fullerenes for efficient polymer solar cells. *Adv. Mater.* **2015**, *27*, 1170–1174.

49 Yuan, J.; Zhang, Y.; Zhou, L.; Zhang, G.; Yip, H. L.; Lau, T. K.; Lu, X.; Zhu, C.; Peng, H.; Johnson, P. A.; Leclerc, M.; Cao, Y.; Ulanski, J.; Li, Y.; Zou, Y. Single-junction organic solar cell with over 15% efficiency using fused-ring acceptor with electron-deficient core. *Joule* **2019**, *3*, 1140–1151.

50 Zhang, Y.; Wan, Q.; Guo, X.; Li, W.; Guo, B.; Zhang, M.; Li, Y. Synthesis and photovoltaic properties of an n-type two-dimension-conjugated polymer based on perylene diimide and benzodithiophene with thiophene conjugated side chains. *J. Mater. Chem. A* **2015**, *3*, 18442–18449.

51 Zhang, M.; Guo, X.; Ma, W.; Ade, H.; Hou, J. A large-bandgap conjugated polymer for versatile photovoltaic applications with high performance. *Adv. Mater.* **2015**, *27*, 4655–4660.

52 Zhang, Y.; Wang, Y.; Yang, T.; Liu, T.; Xiao, Y.; Lu, X.; Yan, H.; Yuan, Z.; Chen, Y.; Li, Y. Thioether bond modification enables boosted photovoltaic performance of nonfullerene polymer solar cells. *ACS Appl. Mater. Interfaces* **2019**, *11*, 32218–32224.

53 Zhang, Y.; Shi, L.; Yang, T.; Liu, T.; Xiao, Y.; Lu, X.; Yan, H.; Yuan, Z.; Chen, Y.; Li, Y. Introducing an identical benzodithiophene donor unit for polymer donors and small-molecule acceptors to unveil the relationship between the molecular structure and photovoltaic performance of non-fullerene organic solar cells. *J. Mater. Chem. A* **2019**, *7*, 26351–26357.

54 Wu, M.; Shi, L.; Hu, Y.; Chen, L.; Hu, T.; Zhang, Y.; Yuan, Z.; Chen, Y. Additive-free non-fullerene organic solar cells with random copolymers as donors over 9% power conversion efficiency. *Chin. Chem. Lett.* **2019**, *30*, 1161–1167.

55 Qiu, B.; Chen, S.; Li, H.; Luo, Z.; Yao, J.; Sun, C.; Li, X.; Xue, L.; Zhang, Z. G.; Yang, C.; Li, Y. A simple approach to prepare chlorinated polymer donors with low-lying HOMO level for high performance polymer solar cells. *Chem. Mater.* **2019**, *31*, 6558–6567.

56 Li, W.; Li, G.; Guo, X.; Wang, Y.; Guo, H.; Xu, Q.; Zhang, M.; Li, Y. A trifluoromethyl substituted wide bandgap conjugated polymer for non-fullerene polymer solar cells with 10.4% efficiency. *J. Mater. Chem. A* **2018**, *6*, 6551–6558.

57 Tang, A.; Song, W.; Xiao, B.; Guo, J.; Min, J.; Ge, Z.; Zhang, J.; Wei, Z.; Zhou, E. Benzotriazole-based acceptor and donors, coupled with chlorination, achieve a high V_{OC} of 1.24 V and an efficiency of 10.5% in fullerene-free organic solar cells. *Chem. Mater.* **2019**, *31*, 3941–3947.

58 Tang, A.; Zhang, Q.; Du, M.; Li, G.; Geng, Y.; Zhang, J.; Wei, Z.; Sun, X.; Zhou, E. Molecular engineering of D-*π*-A copolymers based on 4,8-bis(4-chlorothiophen-2-yl)benzo[1,2-*b*:4,5-*b*′]dithiophene (BDT-T-Cl) for high-performance fullerene-free organic solar cells. *Macromolecules* **2019**, *52*, 6227–6233.

59 Chao, P.; Mu, Z.; Wang, H.; Mo, D.; Chen, H.; Meng, H.; Chen, W.; He, F. Chlorination of side chains: a strategy for achieving a high open circuit voltage over 1.0 V in benzo[1,2-*b*:4,5-*b*']dithiophene-based non-fullerene solar cells. *ACS Appl. Energy Mater.* **2018**, *1*, 2365–2372.
60 Kini, G. P.; Jeon, S. J.; Moon, D. K. Design principles and synergistic effects of chlorination on a conjugated backbone for efficient organic photovoltaics: a critical review. *Adv. Mater.* **2020**, *32*, 1906175.
61 Chao, P.; Johner, N.; Zhong, X.; Meng, H.; He, F. Chlorination strategy on polymer donors toward efficient solar conversions. *J. Energy Chem.* **2019**, *39*, 208–216.
62 Yao, H.; Cui, Y.; Yu, R.; Gao, B.; Zhang, H.; Hou, J. Design, synthesis, and photovoltaic characterization of a small molecular acceptor with an ultra-narrow band gap. *Angew. Chem. Int. Ed.* **2017**, *56*, 3045–3049.
63 Zhang, Y.; Yao, H.; Zhang, S.; Qin, Y.; Zhang, J.; Yang, L.; Li, W.; Wei, Z.; Gao, F.; Hou, J. Fluorination vs chlorination: a case study on high performance organic photovoltaic materials. *Sci. China Chem.* **2018**, *61*, 1328–1337.
64 Ma, R.; Liu, T.; Luo, Z.; Guo, Q.; Xiao, Y.; Chen, Y.; Li, X.; Luo, S.; Lu, X.; Zhang, M.; Li, Y.; Yan, H. Improving open-circuit voltage by a chlorinated polymer donor endows binary organic solar cells efficiencies over 17%. *Sci. China Chem.* **2020**, *63*, 325–330.
65 Luo, Z.; Bin, H.; Liu, T.; Zhang, Z. G.; Yang, Y.; Zhong, C.; Qiu, B.; Li, G.; Gao, W.; Xie, D.; Wu, K.; Sun, Y.; Liu, F.; Li, Y.; Yang, C. Fine-tuning of molecular packing and energy level through methyl substitution enabling excellent small molecule acceptors for nonfullerene polymer solar cells with efficiency up to 12.54%. *Adv. Mater.* **2018**, *30*, 1706124.
66 Gao, W.; Zhang, M.; Liu, T.; Ming, R.; An, Q.; Wu, K.; Xie, D.; Luo, Z.; Zhong, C.; Liu, F.; Zhang, F.; Yan, H.; Yang, C. Asymmetrical ladder-type donor-induced polar small molecule acceptor to promote fill factors approaching 77% for high-performance nonfullerene polymer solar cells. *Adv. Mater.* **2018**, *30*, 1800052.
67 Xie, D.; Liu, T.; Gao, W.; Zhong, C.; Huo, L.; Luo, Z.; Wu, K.; Xiong, W.; Liu, F.; Sun, Y.; Yang, C. A novel thiophene-fused ending group enabling an excellent small molecule acceptor for high-performance fullerene-free polymer solar cells with 11.8% efficiency. *Solar RRL* **2017**, *1*, 1700044.
68 Guo, Q.; Ma, R.; Hu, J.; Wang, Z.; Sun, H.; Dong, X.; Luo, Z.; Liu, T.; Guo, X.; Guo, X.; Yan, H.; Liu, F.; Zhang, M. Over 15% efficiency polymer solar cells enabled by conformation tuning of newly designed asymmetric small-molecule acceptors. *Adv. Funct. Mater.* **2020**, 2000383.

https://doi.org/10.1007/s10118-020-2435-5